

휴머노이드 로봇의 뉴럴네트워크 제어

Neural Network Control of Humanoid Robot

김 동 원*, 김 낙 현, 박 귀 태
(Dong W. Kim¹, Nak-Hyun Kim², and Gwi-Tae Park³)

¹Inha Technical College

²Hyundai Mobis

³Korea University

Abstract: This paper handles ZMP based control that is inspired by neural networks for humanoid robot walking on varying sloped surfaces. Humanoid robots are currently one of the most exciting research topics in the field of robotics, and maintaining stability while they are standing, walking or moving is a key concern. To ensure a steady and smooth walking gait of such robots, a feedforward type of neural network architecture, trained by the back propagation algorithm is employed. The inputs and outputs of the neural network architecture are the ZMPx and ZMPy errors of the robot, and the x, y positions of the robot, respectively. The neural network developed allows the controller to generate the desired balance of the robot positions, resulting in a steady gait for the robot as it moves around on a flat floor, and when it is descending slope. In this paper, experiments of humanoid robot walking are carried out, in which the actual position data from a prototype robot are measured in real time situations, and fed into a neural network inspired controller designed for stable bipedal walking.

Keywords: neural network, humanoid robot control, ZMP (Zero Moment Point)

I. 서론

Throughout history, the human body and mind have inspired artists, engineers, and scientists. The field of humanoid robotics focuses on the creation of robots that are directly inspired by human capabilities. These robots usually share similar kinematics to humans, as well as similar sensing and behavior. The motivations that have driven the development of humanoid robots vary widely [1]. The primary motives are expected to assist human beings, cooperate with people and be stable enough not to fall down to avoid hurting nearby humans, other objects as well as damaging their own bodies. Keeping the humanoid robots stable and steady when they are standing, walking or moving is one of the fundamental functions and most important issue that needs to be addressed. To handle this important issue, many intelligent control schemes have been proposed [2-5]. However, most of these proposed schemes have produced restricted simulation results only, and so it is difficult to analyze the real stabilities of actual humanoid robots based on their walking patterns.

As for the indices of biped walking robots to improve robotic stability, the zero moment point (ZMP) has been introduced and is commonly used for the gait planning of biped humanoid robots. This is a key point in the control of ASIMO [6], a 26-DOF humanoid robot developed by Honda Motor Company in 2000. Vukobratovic et al., [7] investigated the walking dynamics and has proposed ZMP as a good index for walking stability. Kim et al. [8,9] employed various computational intelligence methods to

design a model of robotic locomotion based on the determination of the ZMP trajectories. The ZMP, which is defined as the point on the ground about which the sum of all the moments of the active forces equals zero, is indispensable in ensuring dynamic stability of a biped robot. If the ZMP is inside the ground support polygon, then the biped robot maintains its dynamic balance. When the ZMP reaches an edge of the support polygon, the robot becomes unstable and will tend to rotate around that edge. If the ZMP falls outside the support polygon, the robot cannot be dynamically stable, and so will fall down unless controlled dynamically to maintain some desired motions. As a result, the ZMP trajectories are used as a reference for stable walking in humanoid robots.

In this paper, a prototype humanoid robot is designed, and ZMP humanoid robot control based and inspired on neural network is demonstrated. Because the neural network is learning from idealized ZMP trajectories, the detailed modeling procedures for ensuring the stability of the robot and the physical errors from the mechanical points of view are not required. From the experimental results, the prototype humanoid robot system shows good balance using the designed neural network controller thereby demonstrating and verifying the controller's performance.

II. HUMANOID ROBOT SYSTEM AND ITS ZMP

A biped humanoid robot is designed and implemented. The robot has 19 joints, and the locations of the joints for performing the required motions are shown in Fig. 1 in that there are three degree of freedoms (DOF) are assigned to each arm, three and two DOFs are assigned to the hip and the ankles, respectively, and one to each of the two knees. The height and total weight are about 325mm and 1,500g, including the batteries. Each joint is driven by a RC servomotor, consisting of a DC motor, a gear, and a simple controller. Each of the RC servomotors is mounted in the

* 책임저자(Corresponding Author)

논문접수: 2010. 6. 10., 수정: 2010. 7. 12., 채택확정: 2010. 7. 20.

김동원: 인하공업전문대학 디지털 전자과(dwnkim@inhac.ac.kr)

김낙현: 현대모비스 기술연구소 플랫폼설계 2팀(vester@mobis.co.kr)

박귀태: 고려대학교 공과대학 전기공학과(gtspark@korea.ac.kr)

※ 이 논문은 2010학년도 인하공업전문대학 교내연구비지원에 의하여 연구되었음.

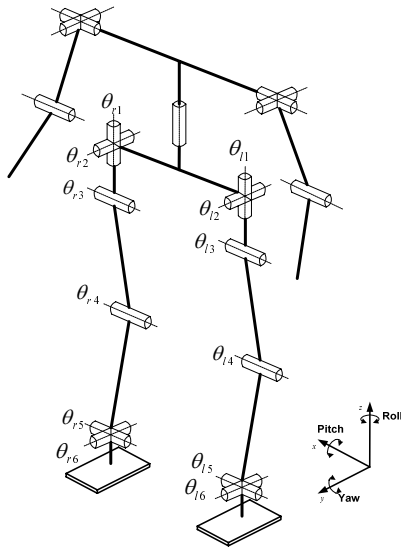


그림 1. 휴머노이드 로봇의 조인트 각도표시.
Fig. 1. Joint angle representation of humanoid robot.

표 1. 휴머노이드 로봇의 사양.
Table 1. Specification of the humanoid robot.

| | |
|----------------------------|--|
| Size | Height : 325mm |
| Weight | 1.5kg |
| CPU | S3C3410X (ARM7 core, 16bit, 40Mhz) embedded in robot |
| Actuator (RC Servo motors) | HS-5945MG (Torque : 11kg·cm at 4.8V) |
| Degree of freedom | 19 DOF (Leg+Arm+Waist)= 2*6 + 3*2+1 |
| Power source | Battery |
| Actuator | AA Size Ni-Cd (6V, 1,100mAh) |
| Control board | AAA size Ni-Cd (7.2V, 250mAh) |

link structure. Each foot is equipped with four force sensors and rubber bushing which protects the sensors and the robot from the touchdown impacts. The specifications of the proposed humanoid robot are given in Table 1 and more detailed information and a block diagram of the robotic system can be found in [8].

As a significant stability criterion of ensuring robotic balance, the ZMP trajectory is used, and the real ZMP is calculated based on the data of the force sensors equipped on each foot. In addition, the ZMP is experimentally obtained for various operating environments, such as a flat floor and ascending on sloped surface. During walking, two different situations arise in sequence: the statically stable double-support phase, in which the robot is supported on both feet simultaneously, and the statically unstable single-support phase, when only one foot of the robot is in contact with the ground while the other is being transferred from the back to front positions so that the locomotion of the robot changes its structure during a single walking cycle. In the ZMP trajectories, the ZMP positions of the humanoid walking robot are under each foot during the single support phases. The ZMP concept has been properly comprehended by researchers and it is widely used and frequently cited. Its interpretation is summarized below and further discussion on the details on the ZMP and the conditions can be found in [10].

Fig. 2 shows the concepts of the ZMP and stability margin, where P is the point at which $T_x = 0$ and $T_y = 0$, and T_x and T_y

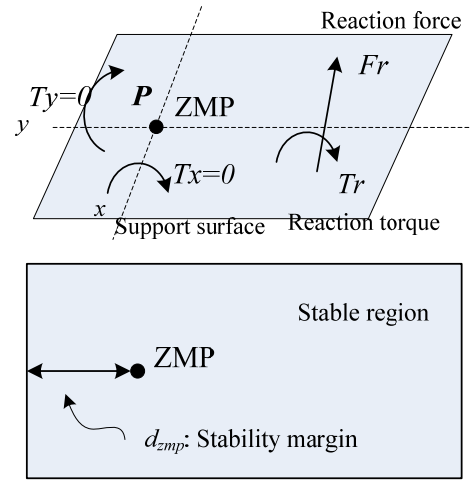


그림 2. ZMP와 안정도 마진에 대한 개념.
Fig. 2. Concept of ZMP and stability margin.

represent the moments around the x - and y -axes, generated by the reaction force F_r and the reaction torque T_r so that the point P is defined as the zero moment point.

When the ZMP exists within the ground support surface, the contact between the ground and the support leg is stable:

$$P_{ZMP} = (x_{ZMP}, y_{ZMP}, 0) \in S$$

where P_{ZMP} denotes the position of the ZMP, and S denotes the domain of the support surface. This condition indicates that no rotation around the edges of the foot occurs.

If the ZMP is within the convex hull of all contact points (the region for stability), the biped robot is able to walk. If the minimum distance between the ZMP and the boundary of the stable region is large, the moment preventing the biped robot from tipping over is also large. The minimum distance d_{zmp} between the ZMP and the boundary of the stability region is called the stability margin [11].

In many studies, the ZMP coordinates are computed using a model of the robot and information from the joint encoders but a more direct approach is employed here using measurement data from sensors mounted at the robot feet. Fig. 3 illustrates the positions of the force sensors on the two feet. The type of force

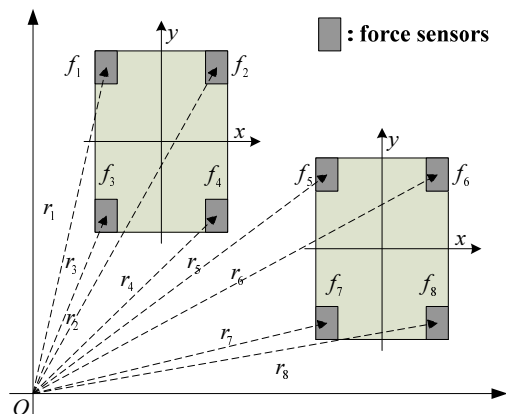


그림 3. 발바닥에 위치한 힘센서의 분산형태
Fig. 3. Distribution of the force sensors on the feet.

sensor used in the experiments is the FlexiForce sensor A201 which are attached to the four corners of the sole plates, and measurements are carried out in real-time. The foot pressure is obtained by summing the force signals and it is easy to calculate the actual ZMP from this force sensor data. The feet support phase ZMPs in the local foot coordinate frame are computed by

$$P = \frac{\sum_{i=1}^8 f_i r_i}{\sum_{i=1}^8 f_i} \quad (1)$$

where f_i is the force applied to the right and the left foot sensors, and r_i is the sensor position, which form vectors and they are also shown in Fig. 3. In the figure, O is the origin of the feet's coordinate frame, which is located in the lower left side of the left foot.

III. NEURAL NETWORK CONTROL

In this section, the neural network (NN) algorithm needed for the biped control is presented. Neural networks have gained popularity as an emerging and effective computational technology offering new avenues for exploring the dynamics of many nonlinear applications. NNs have flexible mathematical structures which are capable of identifying complex and nonlinear relationships between the inputs and outputs of system data sets and their architectures are now widely acknowledged to offer useful and efficient methods, particularly in problems where the characteristics of the processes are difficult to describe by physically reasoned equations. For more detailed descriptions refer to the Refs [12,13].

The topology of any NN determines the accuracy and the domain of representation of a particular NN model. Therefore, the determination of the numbers of hidden layers and neurons in the hidden layer is more arbitrary and application-dependent. In this paper, a single hidden layer is considered, and ten neurons in the hidden layer are determined. For a given training set of input-output pairs (\mathbf{x}, \mathbf{d}) , the back-propagation algorithm performs two phases of data flow. First, the input pattern \mathbf{x} is propagated from the input layer to the output layer and, as a result of this forward flow of data, it produces a predicted output \mathbf{y} . Then, the error signals resulting from the difference between \mathbf{d} and \mathbf{y} are back-propagated from the output layer to the previous layers, which then update their weights. The detailed back-propagation

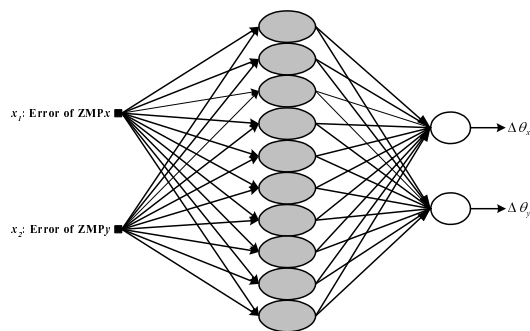


그림 4. 휴머노이드 로봇제어를 위한 뉴럴네트워크의 구조.
Fig. 4. Architecture of the neural network for the humanoid robot controller.

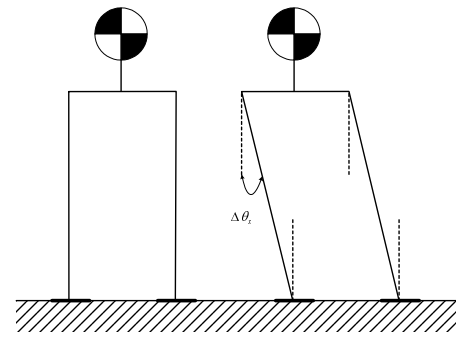


그림 5. 질량 M을 가진 휴머노이드 로봇의 간략화된 그림.
Fig. 5. Simplified humanoid robot with mass M.

algorithm can be found in [13]. As seen from Fig. 4, 2, 10 and 2 processing elements in the input layer, the hidden layer and the output layer, are considered based on the trial-and-error method. The errors of the ZMP trajectories, as x - and the y -coordinates are input into the input layer, and the compensation angles of the x - and the y -coordinates for the humanoid robot walking are output from the network.

To design the ZMP based neural network controller, the humanoid robot is simplified as having a mass M moving like an inverted pendulum, as shown in Fig. 5.

If the humanoid robot is proceeding in the forward direction without falling down, its center of mass (CoM) is shifting gradually. At this moment, the joints in the left and right feet, $\theta_{l2}, \theta_{l6}, \theta_{r2}, \theta_{r6}$ driven identically have a very important role. These joints in the hip and ankle of the robot are for yawing motions which maintain the balance of the robot while standing and walking. By compensating the joint angle $\Delta\theta_x$ to these yawing joints, the CoM of the robot, varying in the right and left portions will adjust the overall position of the robot. The joints θ_{l3}, θ_{r3} in the hip are responsible for pitching of the robot which keeps the upper body of the robot upright when walking. The joint angle $\Delta\theta_y$ can also be compensated for by the pitching joints so that the CoM of the robot will vary from being behind and in front. The adjusted position of the robot, and its corresponding upright, are tuned from the controller gradually. Finally a reasonable trajectory of the ZMP can be obtained from the walking humanoid robot by correcting the values $\Delta\theta_x, \Delta\theta_y$. The obtained ZMP is compared with the desired ZMP, and their errors are employed as input data for the neural network controller.

The ZMP based neural network controller is depicted in Fig. 6 where by using the predefined footstep and its height, the walking pattern for the robot is made, and each of the 19 actuators work to follow the desired pattern. Then the humanoid robot starts to move and the four force sensing resistor (FSR) sensors on each foot measure the force signals in real-time, and the foot pressure is obtained; from this force sensor data, the ZMP of the robot is calculated using Equ. 1 and after calculating the actual ZMP of the humanoid robot, it is compared with the desired one. The differences between the two are used as input data for the neural network controller, which makes the yawing and the pitching joint signals follow the desired ZMP. The inputs and outputs of the neural network, having it architecture as two inputs, two outputs, and 10 nodes in the hidden layer are the errors of the ZMP

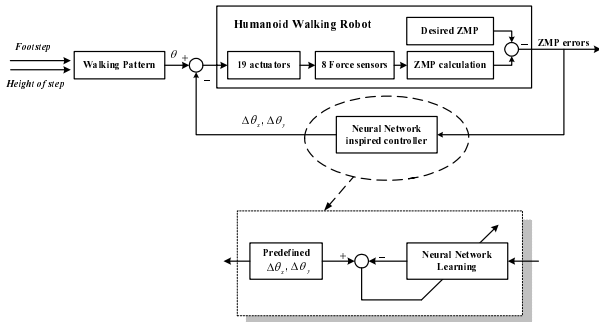


그림 6. NN제어와 학습단계.

Fig. 6. NN controlling and learning phase.

trajectories, the x - and y -coordinates and the $\Delta\theta_x$, $\Delta\theta_y$ angles, respectively.

IV. EXPERIMENTAL RESULTS

This section discusses the performance of the proposed controller for humanoid robot walking where the experimental results have been obtained for the situation shown in Fig. 7 in which a real humanoid robot has been considered.

Using RS-232 communication, the operational signals, the sensor values, and the ZMP location are being transmitted and received between the computer and the humanoid robot. A 40Mhz, 16bit microcontroller carries out an important role in generating the control signal for each joint in the RC servomotors, and carries out the sampling procedure from the FRS sensors on the feet, calculates the ZMP trajectories and the $\Delta\theta_x$, $\Delta\theta_y$ angles from the neural network, and transmits the calculated ZMP values to the computer via the RS-232 communication. The values from the FRS sensors on each foot are sampled by a 10bit, 8channel A/D

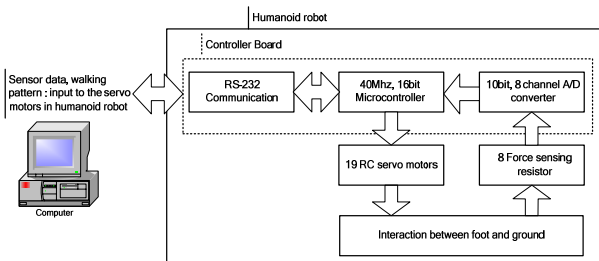


그림 7. 휴머노이드 로봇을 위한 실험환경 셋업.

Fig. 7. Experimental setup for the humanoid robot.

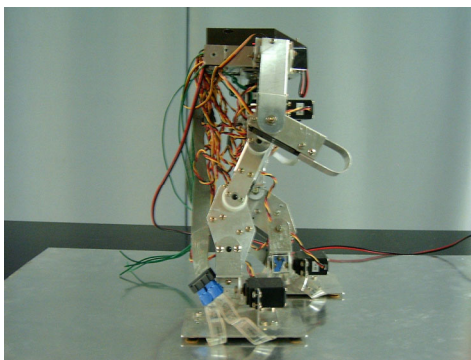


그림 8. 평지를 보행하는 휴머노이드 로봇.

Fig. 8. Humanoid robot walking on flat floor.

converter, with a 50ms cycling interval on the control board.

The walking motions of the humanoid robot on flat ground are shown in Fig. 8. The proposed humanoid robot is able to walk one step of length 48 mm per 1.4s on flat floor. In Fig. 9, the corresponding ZMP trajectories are shown for walking on the flat

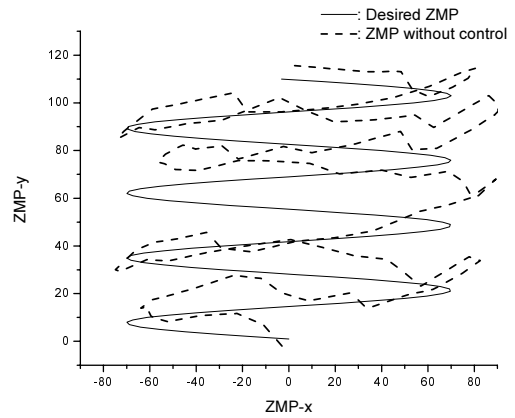


그림 9. 그림 8에 해당되며 제어가 없는 휴머노이드 로봇의 ZMP 궤적.

Fig. 9. ZMP trajectory of the humanoid robot without controller corresponding to Fig. 8.

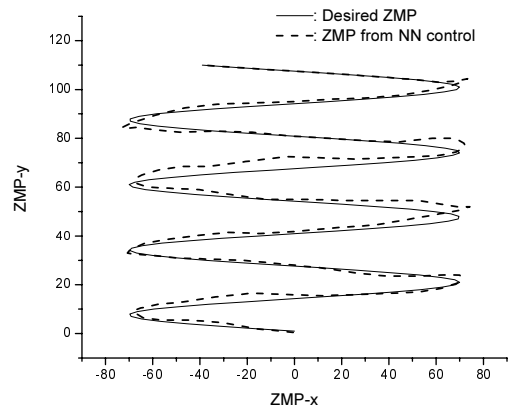


그림 10. 그림 8에 해당되며 NN 제어를 가진 휴머노이드 로봇의 ZMP 궤적.

Fig. 10. ZMP trajectory of the humanoid robot with the NN controller corresponding to Fig. 8.

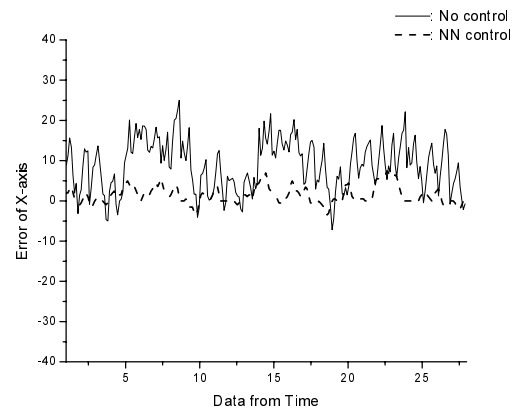


그림 11. 평지를 보행하는 휴머노이드 로봇의 X-축 에러.

Fig. 11. X-axis error of the humanoid robot walking on flat floor.

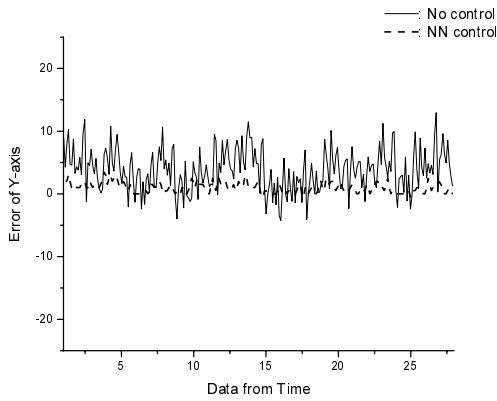


그림 12. 평지를 보행하는 휴머노이드 로봇의 Y-축 에러.
Fig. 12. Y-axis error of the humanoid robot walking on flat floor.

표 2. 평지를 보행하는 휴머노이드 로봇의 정확성 비교.
Table 2. Accuracy of the humanoid robot walking on flat ground.

| Functionality of NN control | x-axis | y-axis |
|-----------------------------|---------|--------|
| Without good control | 10.7973 | 5.0807 |
| With NN inspired control | 2.5060 | 1.2869 |

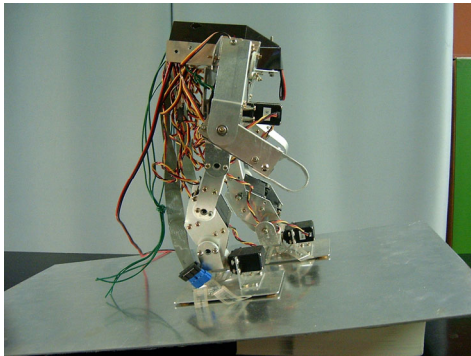


그림 13. 경사면을 보행하는 휴머노이드 로봇.
Fig. 13. Humanoid robot walking on an ascending slope.

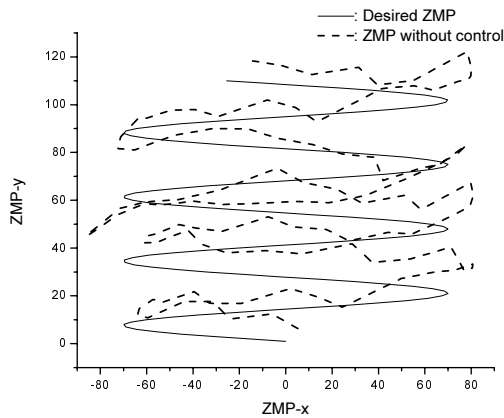


그림 14. 그림 13에 해당되며 제어가 없는 휴머노이드 로봇의 ZMP 궤적.
Fig. 14. ZMP trajectory of the humanoid robot without controller corresponding to Fig. 13.

floor. The humanoid robot should follow the desired ZMP, as shown in the figure but the robot is not able to do this well without effective control whereas when the neural network controller is

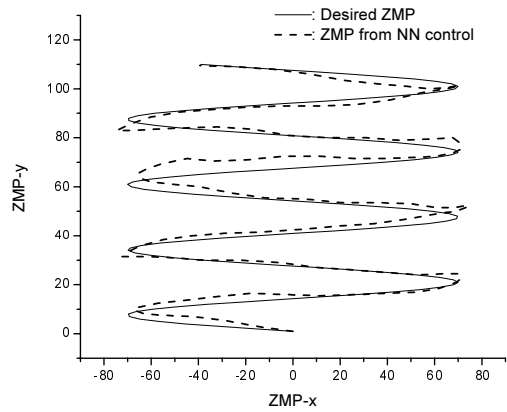


그림 15. 그림 13에 해당되며 NN 제어를 가진 휴머노이드 로봇의 ZMP 궤적.
Fig. 15. ZMP trajectory of the humanoid robot with the NN controller corresponding to Fig. 13.

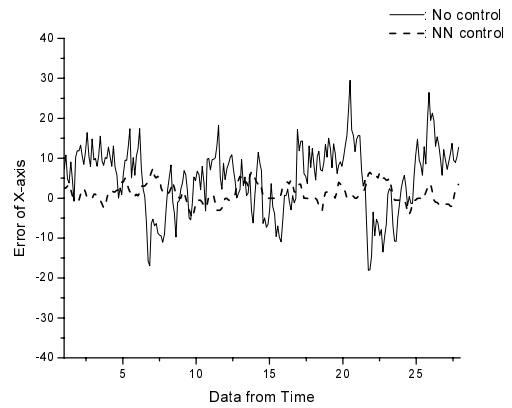


그림 16. 경사면을 보행하는 휴머노이드 로봇의 X-축 에러.
Fig. 16. X-axis error of the humanoid robot walking on an ascending slope.

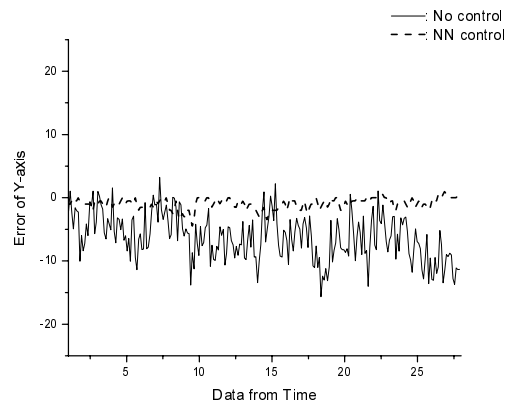


그림 17. 경사면을 보행하는 휴머노이드 로봇의 Y-축 에러.
Fig. 17. Y-axis error of the humanoid robot walking on an ascending slope.

used, the robot tracks the desired ZMP very well. To compare the errors between the two cases, the x- and the y-axes errors of the humanoid robot walking on flat floor are shown in Fig. 12 and Table 2 shows the root mean squared error (RMSE) values corresponding to these cases. The results compare well in respect to demonstrating the effective functionality of the new controller

표 3. 경사면을 보행하는 휴머노이드 로봇의 정확성 비교.
Table 3. Accuracy of the humanoid robot walking on an ascending slope.

| Functionality of NN control | x- axis | y- axis |
|-----------------------------|---------|---------|
| Without control | 9.6741 | 7.2160 |
| With NN controller | 2.6961 | 1.2950 |

developed.

Using the same method, the humanoid robot walking on ascending slope is considered, and the results are shown in the following figures. Fig. 13 shows the side view of the robot walking up sloped surfaces and Fig. 14 shows the corresponding ZMP trajectories of the robot walking without control (the trajectories with control are shown in Fig. 15). To compare the errors from these cases, Fig. 16 presents the x-axis errors and Fig. 17 presents the y-axis errors. Tables 3 presents the RMS errors based on the functionality of the controller for the humanoid robot walking on the ascending slope.

V. CONCLUSIONS

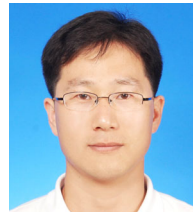
Neural network control for biped humanoid robot has been proposed considering flat floor and sloped surface. A neural network architecture with two inputs, two outputs, and 10 neurons in the hidden layer are considered; the errors of the ZMPx, and the ZMPy of the robot and its x, y positions are taken as the inputs and the outputs of the NN, respectively. To verify the functionality of the NN controller, experiments of a prototype humanoid robot performing walking actions have been carried out; the desired and actual ZMP trajectories with the errors have been also presented for comparing the performance of the NN controller. The experimental results presented demonstrate that the proposed humanoid robot system, with the neural network controller, shows good balance, and verifies that the new controller is able to give satisfactory walking performances.

REFERENCES

- [1] B. Siciliano and O. Khatib (Eds), *Springer Handbook of Robotics*, Springer-Verlag Berlin Heidelberg 2008.
- [2] R. K. Jha, B. Singh, and D. K. Pratihari, "On-line stable gait generation of a two-legged robot using a genetic-fuzzy system," *Robot. Auton. Syst.*, vol. 53, pp. 15-35, 2005.
- [3] S. Murakami, E. Yamamoto, and K. Fujimoto, "Fuzzy Control of Dynamic Biped Walking Robot," *Proc. of the 4th IEE International joint conference on fuzzy systems*, vol. 1, pp. 77-82, 1995.
- [4] H. Wongsuwan and D. Laowattana, "Neuro-fuzzy algorithm for a biped robotic system," *Int. J applied Mathematics and Comp. Sci.*, vol. 3, no. 4, pp. 195-201, 2007.
- [5] M. Y. Shieh, K. H. Chang, and Y. S. Lia, "Design of a biped locomotion controller based on adaptive neuro-fuzzy inference systems," *J. Phys.: Conf. Ser.* vol. 96, pp. 1-8, 2008.
- [6] K. Hirai, M. Hirose, Y. Haikawa, and T. Takenaka, "The development of Honda humanoid robot," *Proc. IEEE Int. Conf. Robotics and Automation*, Leuven, Belgium, vol. 2, pp. 1321-1326, May 1998.
- [7] M. Vukobratovic, B. Brovac, D. Surla, and S. Stokic, *Biped locomotion*, Springer Verlag, New York, NY, 1990.
- [8] D. Kim, S. J. Seo, and G. T. Park, "Zero-moment point trajectory

modeling of a biped walking robot using an adaptive neuro-fuzzy systems," *IET. Control Theory Appl.*, vol. 152, pp. 411-426, 2005.

- [9] D. Kim and G. T. Park, *Advanced Humanoid Robot Based on the Evolutionary Inductive Self-organizing Network*, Humanoid Robots-New Developments, pp. 449-466, 2007.
- [10] M. Vukobratovic and B. Brovac, "Zero-moment point-thirty five years of its life," *Int. J. Humanoid Robotics*, vol. 1, pp. 157-173, 2004.
- [11] Q. Huang, K. Yokoi, S. Kajita, K. Kaneko, H. Arai, N. Koyachi, and K. Tanie, "Planning walking patterns for a biped robot," *IEEE Trans. Robotics Automation*, vol. 17, no. 3, pp. 280-288, 2001.
- [12] J. Jang, C. Sun, and E. Mizutani, *Neuro-Fuzzy and Soft Computing: A Computational Approach to Learning and Machine Intelligence*, Prentice-Hall, 1997.
- [13] C. Lin and C. G. Lee, *Neural Fuzzy Systems: A Neuro-Fuzzy Synergism to Intelligent Systems*, Prentice-Hall, 1996.



김 동 원

2007년 고려대학교 전기공학과(공학박사). 2007년 고려대학교 공학기술연구소 선임연구원 및 연구교수. 2008년 University of California, Berkeley (Prof. Zadeh; BISC Group) Post-Doc., 2009년 University of California, Davis(AHMC Center)

Research Fellow. 2009년~현재 인하공업전문대학 디지털 전자과 교수. 관심분야는 이족 휴머노이드 로봇 설계, 지능 모델링 및 로봇지능, 멀티로봇의 학습 및 응용, 소프트 컴퓨팅 기반 진화된 뉴로-퍼지 시스템 및 이를 이용한 지능제어.



김 낙 현

2004년 고려대학교 전기공학과(공학석사). 현재 현대모비스 기술연구소 플랫폼 품설계2팀 주임연구원. 근무분야는 차량용 멀티미디어 기기 회로설계. 관심분야는 보행로봇, 자율이동 로봇.



박 귀 태

1975년 고려대학교 전기공학과(공학사). 1977년 동 대학원 전기공학과(공학석사). 1981년 동대학원 전기공학과(공학박사). 1978년~1981년 광운대학교 전기공학과 조교수. 1981년~현재 고려대학교 전기전자전파공학부 교수. 1994년

~2000년 대한전기학회 이사 및 평의원. 1994년~1996년 퍼지 시스템학회 이사. 1996년~1998년 제어·자동화·시스템학회 이사. 대한전기학회 및 제어·로봇·시스템학회 Fellow. 2000년~2005년(사) IBS KOREA 회장. 2006년 12월~현재 국토해양부 고층 건물 시공 자동화 연구단장. 관심분야는 진화된 퍼지 및 신경망, 로보틱스, 컴퓨터 비전, 지능제어, 인텔리전트 빌딩 시스템 및 정보통신.